ejpmr, 2017,4(4), 22-33

SJIF Impact Factor 4.161

EUROPEAN JOURNAL OF PHARMACEUTICAL AND MEDICAL RESEARCH

www.ejpmr.com

Research Article

ISSN 2394-3211

EJPMR

DESIGN, SYNTHESIS AND BIOLOGICAL EVALUATION OF MORPHOLINE, PIPERIDINE AND PHENYL DERIVATIVES OF QUINAZOLINONE AS HSP90 ATPASE INHIBITORS

Suby T. Baby[1]*, Shailendra Sharma[1], Sreenivas Enaganti[2] and Roby P. Cherian[3]

[1]Faculty of Pharmaceutical Sciences, Jodhpur National University, Jodhpur, Rajasthan 342003, India.
[2]Averin Biotech, 208, 2ndFloor, Windsor Plaza, Nallakunta, Hyderabad 500044, Telangana, India.
[3]Jazan University, P.O. Box 114, Jazan 45142, Kingdom of Saudi Arabia

***Corresponding Author: Suby T. Baby**

Faculty of Pharmaceutical Sciences, Jodhpur National University, Jodhpur, Rajasthan 342003, India.

Article Received on 01/02/2017 **Article Revised on 22/02/2017** **Article Accepted on 13/03/2017**

ABSTRACT

Hsp90 plays a major role in the oncogenic proteostasis where the over expressed levels of Hsp90 are found in various cancers constituting its role in growth and survival of malignant cells, thus making Hsp90 as an important molecular target in cancer therapeutics. Hence, the discovery and development of novel chemical scaffolds targeting Hsp90, with superior anticancer activity remain an important priority in the cancer field. Here in our study describes the synthesis, biological evaluation of novel quinazolinone derivatives ability to function as anticancer agents on MCF-7 *human* breast cancer cell line by MTT assay and their potential to suppress Hsp90 ATPase activity by Malachite green assay. Further, docking are carried out to know the binding modes of the compounds and validated by structure based pharmacophore modeling studies which reveals the important structural features responsible for ligand binding.

KEYWORDS: Cancer, docking, Hsp90, malignant, pharmacophore, quinazolinone.

1. INTRODUCTION

Heat Shock Protein-90 (Hsp90) is a highly sustainable evolutionary chaperone present in both prokaryotes and eukaryotes and found to play a crucial role in maintaining cellular homeostasis which can be attained by modifying the mis-folded proteins1,2. It accelerates the formation of correct conformations for almost 200 'client' proteins involved in cellular processes such as cell cycle regulation, cell survival, hormone signalling, and act in response to various stresses such as heat, high pressure, and exposure to toxic compounds which triggers the expression of Hsps. These proteins are also expressed and found abundant under non-stress conditions too3,4,5. The function of Hsp90 is complex and involves homodimerization, recruitment of accessory co-chaperones like Hsp70, Hsp40, HOP, AHA1 and p23 with its client proteins like Her2, Raf-1, Akt, Cdk4, polo-1 kinase, B-Raf, HIF-1a, Bcr-Abl, mutant p53 operating in a dynamic 'chaperone cycle' dependent on the ATPase activity of Hsp905,6,7,8. Many of the client proteins act as oncogenic particles which require high Hsp90 activity and consequently lead to cell transformations. As a result, Hsp90 has displayed its pivotal role in oncogenic proteostasis where the over expressed levels of Hsp90 are found in various cancers constituting its role in growth and survival of malignant cells9. Therefore, targeting Hsp90 with chemical inhibitors will degenerate these oncogenic particles and act as anti-cancerous agents providing a promising area of cancer chemotherapy. The inhibitors of Hsp90 deteriorate its client proteins that simultaneously act on several pathways involved in cancer development, without any impact on their cellular counterparts (non-transformed cells) and also reduce the likelihood of the tumor acquiring resistance10,11,12. Additionally, Hsp90 inhibitors have shown higher affinity for cancer cells leading to an increased accumulation of inhibitor in cancer cells6. In general, all the inhibitors of Hsp90 have a common configuration with the N-terminal ATP binding site that has been most widely studied while very less is known about the C-terminal binding site and other middle domains13. Thus through ATP-competitive mechanism of Hsp90 inhibition, many of the inhibitors act by preventing its chaperoning function of ATP to ADP cycling, resulting in the proteasomal degradation of multiple oncogenic clients via the ubiquitin-proteasome pathway and consequently attains antiproliferative activity through the arrest of the tumour growth, morphological and functional differentiation, and activation of apoptosis11,14,15. The combinatorial inhibition markedly reduces the opportunities for cancer cells to develop resistance to Hsp90 inhibition15. To date, none of the Hsp90- targeting agents has received the FDA approval for human use, thus providing space

for exploration of new inhibitors of Hsp90 with increased efficacy and therapeutic potential to treat cancer16.

In the race of new anticancer drug development, heterocyclic compounds, due to their widespread therapeutic uses, have attracted a great deal of attention amongst the scientific community11. Quinazoline derivatives, one of the most significant classes of N-containing fused heterocyclic compounds used in medicine due to their extensive diversity of biological activities and compounds with different substitutions bring together to knowledge of a target with understanding of the molecule types that might interact with the target receptors. Quinazoline compounds are also used in preparation of a variety of functional materials for synthetic medicinal chemistry and also present in many drugs molecules. One of derivative of quinazoline is quinazolinone which is active like quinazoline, have drawn a huge consideration owing to their expanded applications in the field of pharmaceutical chemistry Researchers have already determined many therapeutic activities of these derivatives, including anti-cancer, antiinflammation, anti-bacterial, analgesia, anti-virus, anti-cytotoxin, anti-spasm , anti-tuberculosis, antioxidation, antimalarial, anti-hypertension, anti-obesity, anti-psychotic, anti-diabetes etc.17-27

From our previous work on inhibitors of the Hsp9011, quinazolinone derivatives have shown good binding affinities and strong interactions with the enzyme Hsp90. In continuation of our interest in discovering new antitumor compounds, our ongoing studies on quinazolinone derivatives, we have designed some newly substituted derivatives having phenyl and 4-chlorophenyl moieties containing morpholine and piperidine fragments with propyl spacer group. All the derivatives were synthesized and characterized by IR, 1HNMR and mass spectroscopic studies. The colorimetric assays, malachite green assay) was used to measure the extent of Hsp90 ATPase activity inhibition and MTT assay was used for screening cytotoxic activity on MCF-7 breast cancer cells by our synthesized compounds. Further, docking and pharmacophore studies of the synthesized molecules were carried out with the targeted protein *Human* Heat shock protein-90 (PDB ID: 1YET).

2. MATERIALS AND METHODS

2.1. Chemistry: Melting points of all the compounds was recorded on Casia- Siamia (VMP-AM) melting point apparatus and uncorrected. IR spectra were recorded on a PerkineElmer FT-IR 240-C spectrometer using KBr optics. NMR spectra were recorded on Burker Avance 400 MHz in DMSO-d6 using TMS as internal standard. Electron impact (EI) and chemical ionization mass spectra were recorded on a VG Micromass model 7070H instrument. All the reactions were monitored on silica gel precoated TLC plates of Merck and spots were visualized with UV light. Silica gel used for column chromatography was procured from Merck. All the relevant data regarding characterization of compounds is given Table 1.

2.1.1. Synthesis of 2-mercapto-3-substitutedquinazolin-4(3H)-one (2a-e) from isatoic anhydride & anthranilic acids: Substituted quinozolinones were prepared by the reported procedure28,29. A solution of Aniline (1.0 eq) in dimethyl sulfoxide (5 vol) was stirred vigorously. To this was added carbon disulphide (2 vol) and aqueous sodium hydroxide (2 vol, 20M) dropwise during 30min with stirring. Dimethyl sulfate (1.0 eq) was then added gradually keeping the reaction mixture in freezing mixture with stirring, and the stirring was continued for further 2 h. The reaction mixture was then poured into ice water. The solid obtained was filtered, washed with water, dried, and recrystallized from ethanol. Isatoic anhydride (1.0eq) and the aforementioned prepared N-(Phenyl) methyl dithiocarbamic acid (1.0 eq) were dissolved in ethanol (15 vol). To this anhydrous potassium carbonate (2.5 eq) was added and refluxed for 18 h. The reaction mixture was cooled in ice, and the solid separated was filtered and purified by dissolving in 10% alcoholic sodium hydroxide solution and precipitated by treating with dilute hydrochloric acid. The solid obtained was filtered, washed with water, and dried. It was recrystallized from ethanol to afford required substituted quinazolinones (**2a-c**). (And) A mixture of substituted anthranilic acid (1.0 eq) and (1.0 eq) phenylisothiocyanate in absolute ethanol (15 vol) containing diisopropylethylamine (2.0 eq) was heated under reflux for 6 h. The solvent was removed under reduced pressure and the solid obtained was dried and recrystallized from ethanol to get the quinazolinone derivatives (**2d-e**).

2.1.2 Synthesis of Amido-alkyl bromides (3a,b)

To a stirred solution of 20-amine in dry.dichloromethane (DCM) at 0-50C under nitrogen atmosphere, then added bromopropionyl bromide dropwise. After addition reaction mixture temperature was raised to room tempature and stirred for 6 hours. After reaction mixture was diluted with DCM and washed with sodium bicarbonate followed by water, dried over sodium sulphate and remove the solvent under reduced pressure. The crude product was used to next step without further purification.

2.1.3 Synthesis of 2-((3-oxo-3-(alkyl/aryl-1-yl) alkyl) thio) – 3 - substituted quinazolin-4 (3H)-ones

Synthesis of (**4a-h**)

A solution of 3-(4-phenyl)-2-thioxo-2,3-dihydro-1H-quinazolin-4-one (**2a**) (1.0 eq) and K2CO3 (2.5 eq) in DMF was cooled to 5 0C, then addes amido-alkyl bromide (**3a**) (1.5 eq). The reaction mixture was stirred at room temperature for 36 h. The reaction mixture was was diluted with cold water and extracted solvent was removed under reduced pressure to afford 2-(3-bromo propyl)-3-(phenyl) quinazolin-4-(3H)-one (4a), it was then purified by column chromatography (60-120 silica mesh) using MeOH:Chloroform mobile phase.

Employing the similar procedure as mentioned for **4a**, compounds **4b-j** was obtained from **2a-e** as solids.

Synthesis of (**4i, 4j**)

A mixture of 2-thioxo-3-phenyl-dihydro quinazolinones (**2d,e**) (1.0 eq) and the appropriate freshly prepared phenacyl bromide (**3c**) (1.0 eq) was refluxed in dry acetone (10 vol) in the presence of anhydrous potassium carbonate (2.0 eq) for 24 h. The reaction mixture was then filtered while hot, and the filtrate was evaporated to dryness. The obtained solid was purified by column chromatography.

The reactions are drawn in Scheme 1.

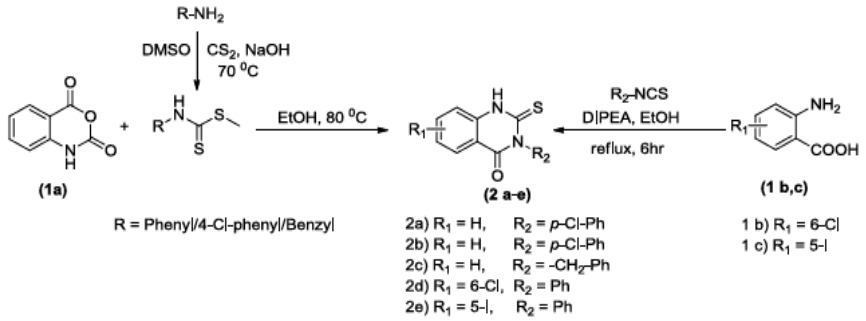

Step 1: Synthesis of 2-mercapto-3-substitutedquinazolin-4(3H)-one (2a-e)

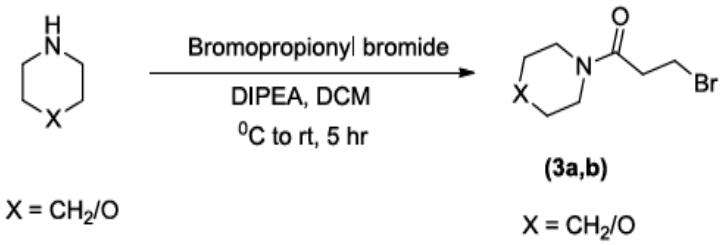

Step 2: Synthesis of Amido-alkyl bromides (3a,b)

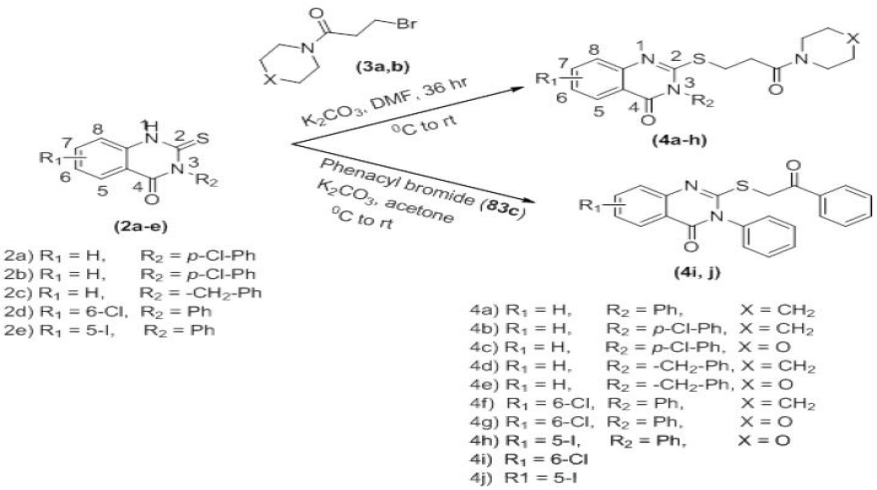

Step 3: Synthesis of 2-((3-oxo-3-(alkyl/aryl-1-yl)alkyl)thio)-3-substitutedquinazolin4 (3H)-ones (4 a-j)

Scheme 1. General scheme of synthesis of the Quinazolinone derivatives

2.2. Molecular docking studies

2.2.1. Ligand Preparation: A dataset of 10 synthesized Quinazolinone derivative 2D structures, were sketched using ACD Chemsketch software and converted to their 3D representation by using catalyst algorithm of Acclerys Discovery Studio (ADS). Prepare ligands module of ADS was used for Ligand preparation which corrects for hydrogen bonds addition, bond lengths, bond angles, isomer and tautomer generation and filters the ligands by removing the duplicate structures. Further followed by minimization and optimization in CHARMm force field with the smart minimizer algorithm till it satisfied with the convergence gradient of 0.001 kcal/mol, for attaining the low energy conformational structures35.

2.2.2. Protein Preparation: The three dimensional crystal structure of Human Heat shock protein-90 with PDB: 1YET in complex with the ligand Geldanamycin was retrieved from the Protein Data Bank36. The complexes bound to the receptor molecule, all the heteroatoms and the non-essential water molecules were removed. Protein preparation is carried out using prepare protein module of DS which executes the merging of hydrogen atoms, assigning bond orders, creating zero order bonds to metal, creating disulfide bonds, fixing of the charges, and orientation of groups were incorporated. Protein structural minimization was carried out with the minimization module by applying the CHARMm forcefield using steepest descent algorithm with a maximum number of 1000 steps at RMS gradient of 0.01. This was continued until the protein satisfied with a convergence gradient of 0.001 kcal/mol36.

2.2.3. Docking

Molecular docking studies were carried out to estimate the scoring function and evaluate protein–ligand interactions in order to predict the binding affinity and activity of the ligand molecule. The docking program LibDock module in Discovery Studio37 have been employed to generate the bioactive binding poses of synthesized quinazolinone derivatives in the active site of protein Hsp90. The active site of the protein was primarily defined based on the coordinates from the reference crystal ligand Geldanamycin.

This ligand was selected to define the position and size of the active site LibDock uses protein site features called 'HotSpots' that are resolved with a grid fixed in active site which counts the hotspot map for polar and apolar cluster and further used for the alignment of the ligand conformations to the protein interaction sites. All other docking and consequent scoring parameters used were kept at their default settings. Finally at the end of the docking process, it returns all the minimized ligand poses and their rankings. Among all the obtained poses of each ligand, the ligand binding in a receptor cavity is evaluated based on the LibDock top score, which uses a simple pair-wise method. The ligands with high LibDock scores are preferred for estimating binding energies of the protein-ligand complex. The complex pose with the best binding energy is used for further binding mode analysis. In addition, all docked poses were
scored by applying Analyze Ligand Poses sub protocol in Discovery Studio.

2.2.4 Validation of Docking Studies by Structure based Pharmacophore mapping

2.2.4.1 Generation of structure-based pharmacophore model

To further identify the critical structural features of the protein that was important for the ligand binding, structure-based pharmacophore modeling was employed based on the protein ligand complexes. This molecular modeling was carried out to construct a hypothetical pharmacophore model aiming to study fitting of the designed compounds to the generated pharmacophores of our target protein Human Hsp90.

All pharmacophore modeling studies was performed using Catalyst in DS. To build the pharmacophore model for screening, corresponding possible interaction points from active site of Human Hsp90 protein (PDB: 1YET) was generated using the 'Interaction Generation' protocol implemented in Discovery Studio. It extracted all the available hydrophilic and lipophilic interaction points that can be complemented by the inhibitor. The parameters for both 'Density of Lipophilic Sites' and 'Density of Polar Sites' were defined as 10. The active site was then analysed for hydrogen bond donors, acceptors, and hydrophobic features by generating pharmacophore query from the Ludi interaction maps38. During pharmacophore generation a minimum of 1 and a maximum of 2 pharmacophore feature such as hydrogen bond donor (HBD), hydrogen bond acceptor (HBA), and hydrophobic (HY) were included.

Using Edit and Cluster pharmacophore tools, these features were then clustered and the most representative features with catalytic importance were selected and included in the pharmacophore hypothesis. After these operations, a structure-based pharmacophore model comprising the most important pharmacophoric features was built. The final pharmacophore model was subjected to validation based on the active site orientation of inhibitors.

2.2.4.2 Validation of the Pharmacophore

To validate the generated structure-based pharmacophore model, the heterocyclic derivatives are mapped onto the pharmacophore model. This was done by Ligand pharmacophore mapping protocol of DS with the Best Flexible Search option for conformational analysis of each compound with low energies.

Maximum Omitted Features option was chosen as 2 because mapping all the features present in the structure-based hypothesis will reduce the hit rate. The predictive ability of the model was analyzed based on the best fit values that indicate how well the compounds were mapped onto the pharmacophoric features. Compounds were ranked based on fit values. A higher fit value represents a better fit.

2.3 *Malachite Green Assay for Hsp90 ATPase Activity*

ATPase activity was measured by Phosphate hydrolysis using Malachite Green reagent. 1μM Hsp90 was incubated for 2.5 hours at 370C with 0.2mM ATP and Solvent Control (DMSO). After incubation, a Malachite Green reagent was added, followed by quenching with 34% sodium citrate. The absorbance was measured at 620nm in a Specrostar Nano Plate Reader, Germany 30, 31.

Different Concentrations of Standard Hsp90 was taken for comparison of test samples with the standard.

After adding of all the reagents followed by quenching with 34% sodium citrate absorbance was measured at 620nm and test samples were compared to know the concentration of Hsp90 present in the samples. The IC50 values for these compounds under optimized conditions were determined from a range of inhibitor concentrations (0.1–100 μM).

2.4 In vitro cytotoxicity activity

2.4.1 Culture of the MCF-7 breast cancer cells

The MCF-7 breast adenocarcinoma cancer cell line were purchased from NCCS, Pune and the cells were maintained in MEM supplemented with 10% FBS (fetal bovine serum) and the antibiotics penicillin/streptomycin (0.5 mL-1) and cultivated in a humidified incubator at 370C and 5% CO2.

2.4.2. MTT Assay for determination of anticancer activity: The MTT [3-(4, 5-dimethylthiazol- 2-yl)-2,5-diphenyl tetrazolium bromide] based cell proliferation assay method was used to measure the cytotoxic activities of 10 synthesized Quinazolinone derivatives on the MCF-7 cell line. This colorimetric assay measures the reduction of yellow 3-(4,5-dimethythiazol- 2-yl)-2,5-diphenyl tetrazolium bromide (MTT) into to water-soluble, dark purple coloured formazan crystals.

MCF- 7 cells were trypsinized and preform the the tryphan blue assay to know viable cells in cell suspension. Cells were counted by haemocytometer and seeded at density of 5.0 X 103 cells / well in 100 μl media in 96 well plate culture medium and incubated overnight at 370C. The cells were then incubated for another 48 h with various concentrations of test compound in represntive wells in 96 plates. After 48 hrs., Discard the drug solution and add the fresh media with MTT solution (0.5 mg / mL-1) was added to each well and plates were incubated at 370C for 3 hrs. At the end of incubation time, precipitates are formed as a result of the reduction of the MTT salt to chromophore formazan crystals by the cells with metabolically active mitochondria. The optical density of solubilized crystals in DMSO was measured at 570 nm on a microplate reader. The percentage growth inhibition was calculated and concentration of test drug needed to inhibit cell growth by 50% values is generated from the dose-response curves for cell line using with origin software32, 33, 34.

3. RESULTS AND DISCUSSION

3.1. Chemistry: A series of 2-mercapto-3-substituted quinazolin-4(3H)-one derivatives (**4a-j**) involves in three steps. In the first step, synthesis of 2-mercapto-3-substitutedquinazolin-4(3H)-one (2a-e) can be achieved either using isatoic anhydride or by using anthranilic acid. Aniline treated with carbon disulphide and sodium hydroxide in dimethyl sulfoxide (DMSO) to give sodium dithiocarbamate, which was methylated with dimethyl sulfate to afford the dithiocarbamic acid methyl ester. Dithiocarbamic acid methyl ester on reflux with isatoic anhydride (**1a**) in absolute ethanol yielded the desired 3-(phenyl)-2-thioxo-2,3-dihydro-1H-quinazolin-4- one (**2a**). The use of DMSO as the reaction solvent enhanced the rate of reaction, and the use of alkali in higher concentration helped prevent the hydrolysis of the intermediate, probably because of less solvation. Synthesis of 2-mercapto-3-substituted quinazolin-4(3H)-one derivatives (**2a-e**) was achieved by the reaction of a mixture of substituted anthranilic acid (**1b,c**) and phenylisothiocyanate in absolute ethanol containing diisopropylamine was heated under reflux to get the 2-mercapto-3-substitutedquinazolin-4(3H)-ones (**2a-e**). In the second step, 20-amine was reacted with bromopropionylbromide in the presence of diisopropylamine to get the required amido-alkyl compounds (**3a,b**). In the final step, the required 2-((3-oxo-3-(alkyl/aryl-1-yl)alkyl)thio)-3-substitutedquinazolin-4(3H)-ones (**4a-j**) compounds were synthesized by the reacting with corresponding alkyl bromides (**3a,b**) in the presence of potassium carbonate. All the final derivatives are synthesised in quantitative yields. All the derivatives were characterized by 1H, 13C NMR, IR and ESI-MS spectra.

3.1.1. 2-((3-oxo-3-(piperidin-1-yl)propyl)thio)-3-phenyl quinazolin 4(3H)-one (4a): Off white solid, yield 50%, m.p: 155-158 0C, IR (KBr, cm-1): 3377, 1710, 1594 & 1499. 1H-NMR (DMSO-d6, 400 MHz) δ: 7.94 (d, *J* = 7.2 Hz, 1H), 7.75 (d, *J* = 8.0, 2.8 Hz, 1H) and 7.44 (t, J = , 2H), 7.52 (m, 2H) and 7.3 (m, 3H), 3.41(m, 4H) to 3.31 (m, 2H), 2.73 (t, J = Hz, 2H), 1.52 (m, 4H), 1.39 (m, 2H). 13C-NMR (DMSO-d6, 100.6 MHz) δ: 174.74, 164.52, 162.63, 144.94, 135.25, 132.45, 129.79, 128.8, 127.15, 125.29, 122.5, 121.7, 121.09, 48.19, 30.36, 27.52, 23.74 & 22.98. ESIMS: m/z 394 [M+H]+.

3.1.2. 3-(4-chlorophenyl)-2-((3-oxo-3-(piperidin-1-yl)propyl)thio) quinazolin-4(3H)-one (4b): White solid, yield-45%, m.p: 167-170 0C, IR (KBr, cm-1) 3430, 1726, 1601 & 1511. 1H-NMR (DMSO-d6, 400 MHz) δ: 7.96-7.94 (dd, J = 9.2, 8.0 Hz, 1H), 7.50-7.48 (d, J = 7.6 Hz, 2H), 7.48-7.33 (m, 2H), 7.29-7.27 (d, J = 8.4 Hz, 2H), 3.46-3.42 (m, 6H), 2.28-2.77 (m, 4H), 1.57-1.52 (m, 2H), 1.46-1.36 (m, 4H). 13CNMR (DMSO-d6, 100.6 MHz) δ: 173.72, 163.29, 160.01, 147.53, 133.7, 130.51, 129.27, 128.09, 127.23, 123.46, 121.5, 120.75, 49.71, 33.54, 27.49 & 24.72. ESIMS: m/z 445 [M+H2O]+.

3.1.3. 3-(4-chlorophenyl)-2-((3-morpholino-3-oxopropyl)thio) quinazolin-4(3H)-one (4c): White solid, yield-45%, m.p: 145-150 0C, IR (KBr, cm-1) 2924, 1721, 1606 & 1444. 1H-NMR (DMSO-d6, 400 MHz) δ: 8.06 (d, J = 7.6 Hz, 1H), 7.65 (d, J = 7.2 Hz, 1H), 7.47 (m, 3H), 7.29 (m, 3H), 3.53-3.50 (m, 4H), 3.41-3.39 (m, 6H), 2.76-2.73 (t, J = 14.4, 10.0 Hz, 2H). 13C-NMR (DMSO-d6, 100.6 MHz) δ: 169.88, 165.48, 160.01, 145.53, 135.4, 132.42, 130.21, 129.27, 128.09, 127.23, 123.46, 121.5, 120.15, 63.97, 55.64, 30.41 & 27.49. ESIMs: m/z at 429 [M]+.

3.1.4. 3-benzyl-2-((3-oxo-3-(piperidin-1-yl)propyl) thio) quinazolin-4(3H)- one (4d): White solid, yield-55%, m.p: 175-177 0C, IR (KBr, cm-1) 3080, 1702, 1605, 1518 7 1403. 1H-NMR (DMSO-d6, 400 MHz) δ: 7.95 (dd, J = 9.2, 8.0 Hz), 7.79-7.74 (m, 1H), 7.43 (d,J = 7.6 Hz, 1H), 7.37-7.27 (m, 5H), 7.23 (m, 1H), 5.67 (s, 2H), 3.46-3.42 (m, 6H), 2.78 (t, J = 6.8, 13.6 Hz, 2H), 1.57-1.52 (m, 2H), 1.46-1.36 (m, 4H) . 13C-NMR (DMSO-d6, 100.6 MHz) δ: 175.5, 160.25, 155.35, 148.3, 141.34, 133.5, 130.46, 129.57, 128.48, 126.43, 123.97, 120.4, 46.68, 44.18, 33.07, 28.97, 26.9 & 26.14. ESIMS: m/z 408 [M+H]+.

3.1.5.3-benzyl-2-((3-morpholino-3-oxopropyl)thio)quinazolin-4(3H)-one (4e): White solid, yield-55%, m.p: 160-162 0C, IR (KBr, cm-1) 2923, 1708, 1601, 1521 & 1343. 1H-NMR (DMSO-d6, 400 MHz) δ: 7.94 (dd, J = 9.2, 8 Hz, 1H), 7.75 (m, 1H), 7.41 (d, J = 8.0 Hz, 1H, 7.34-7.28 (m, 5H), 7.24 (m, 1H), 5.68 (s. 2H), 3.53-3.52 (m, 4H), 3.41-3.33 (m, 6H), 2.76 (t, J = 12.5, 6.4 Hz, 2H). 13C-NMR (DMSO-d6, 100.6 MHz) δ: 172.1, 162.47, 153.21, 143.08, 140.68, 134.12, 129.24, 127.63, 127.08, 122.8, 121.76, 64.65, 47.46, 44.85, 33.44, 32.71 & 24.73. ESIMS: m/z 432 [M+Na]+.

3.1.6. 6-chloro-2-((3-oxo-3-(piperidin-1-yl)propyl)thio)-3-phenyl quinazolin-4(3H)-one (4f): White solid, yield-55%, m.p: 200-203 0C, IR (KBr, cm-1) 2924, 1708, 1606, 1541 & 1408. 1H-NMR (DMSO-d6, 400 MHz) δ: 8.06 (d, J = 8.4 Hz, 1H), 7.64 (d, J = 2.0 Hz, 1H), 7.56-7.54 (m, 3H), 7.5 (m, 1H), 7.42 (m, 2H), 3.38 (m, 4H), 3.33 (m, 2H), 2.73 (t, J = 13.6, 6.8 Hz, 2H), 1.55 (m, 2H), 1.46-1.39 (m, 4H). 13CNMR (DMSO-d6, 100.6 MHz) δ: 172.57, 166.3, 164.52, 142.46, 135.25, 132.45, 130.89, 128.8, 122.49, 121.69, 121.05, 48.19, 30.36, 27.52, 23.74 & 22.98. ESIMS: m/z 428 [M+H]+.

3.1.7. 6-chloro-2-((3-morpholino-3-oxopropyl)thio)-3-phenyl quinazolin-4(3H)-one (4g): White solid, yield-55%, m.p: 180-185 0C, IR (KBr, cm-1) 2923, 1686, 1554 & 1430. 1H-NMR (DMSO-d6, 400 MHz) δ: 8.06 (d, J = 8.8 Hz, 1H), 7.56 (dd, J = 7.2, 5.6 Hz, 1H), 7.5-7.46 (m, 3H), 7.33-7.24 (m, 2H), 3.53 (d, J = 4.4 Hz, 4H), 3.4-3.33 (m, 6H), 2.76 (t, 13.6, 6.8 Hz, 2H). 13C-NMR (DMSO-d6, 100.6 MHz) δ: 174.64, 166.3, 160.35, 144.17, 135.25, 132.25, 132.45, 130.89, 128.8, 125.28, 122.49, 121.69, 121.05, 68.13, 47.51, 32.45 & 26.78. ESIMS: m/z 408 [M+H]+.

3.1.8. 5-iodo-2-((3-morpholino-3-oxopropyl)thio)-3-phenyl quinazolin -4(3H)-one (4h): White solid, yield-55%, m.p: 140-143 0C, IR (KBr, cm-1) 3213, 1686, 1568 & 1364. 1H-NMR (DMSO-d6, 400 MHz) δ: 7.73-7.7 (dd, J = 10.8, 8.8 Hz, 1H), 7.56-7.55 (m, 2H), 7.41-7.34 (m, 4H), 7.7-6.94 (m, 3H), 3.5.-3.5 (m, 4H), 3.41-3.39 (m, 6H), 2.74 (t, J = 13.6, 7.2 Hz, 2H). 13C-NMR (DMSO-d6, 100.6 MHz) δ: 173.51, 163.02, 161.88, 146.7, 136.71, 136.49, 135.45, 133.77, 129.6, 124.43, 123.27, 121.93, 101.4, 68.04, 45.6, 33.3 & 26.97. ESIMS: m/z 544 [M+Na]+.

3.1.9 Synthesis of 4i, 4j

A mixture of 2-thioxo dihydroquinazolinones **2d,e** (1. 0 eq) and the appropriate freshly prepared phenacyl bromide (**3c)** (1. 0 eq) was refluxed in dry acetone (10 vol) in the presence of anhydrous potassium carbonate (2.0 eq) for 24 h. The reaction mixture was then filtered while hot, and the filtrate was evaporated to dryness. The obtained solid was purified by column chromatography.

3.1.9.1 6-chloro-2-((2-oxo-2-phenylethyl)thio)-3-phenylquinazolin 4(3H)-one (4i): White solid, yield-55%, m.p: 198-201 0C, IR (KBr, cm-1) 2922, 1708, 1602 & 1501. 1H-NMR (DMSO-d6, 400 MHz) δ: 8.08 (d, J = 3.2 Hz 2H), 8.03 (J = 8.4 Hz, 1H), 7.75 (m, 1H), 7.62-7.58 (m, 6H), 7.51-7.44 (m, 4H), 7.06 (d, J = 2.0 Hz, 1H), 4.75 (s, 2H). 13C-NMR (DMSO-d6, 100.6 MHz) δ: 193.14, 165.65, 162.36, 146.86, 137.16, 135.69, 133.57, 132.42, 130.16, 129.4, 128.25, 127.74, 124.55, 121.9, 120.98 & 36.36. ESIMs: m/z 424 [M+H2O]+.

***3.1.9.2 5-iodo-2-((2-oxo-2-phenylethyl)thio)-3-phenylquinazolin4(3H)-one (4j*)**: White solid, yield-55%, m.p: 167-172 0C, IR (KBr, cm-1) 3245, 1696, 1602 & 1551, 1H-NMR (DMSO-d6, 400 MHz) δ: 7.96-7.94 (dd, J = 9.2, 8.0 Hz, 1H), 7.8-7.76 (m, 1H), 7.5-7.46 (m, 4H), 7.44-7.7.3 (m, 3H), 7.31 (m, 3H), 7.29-7.27 (m, 3H), 4.33 (s, 2H). 13C-NMR (DMSO-d6, 100.6 MHz) δ: 194.39, 166.3, 164.52, 144.17, 139.76, 137.95, 135.25, 134.9, 132.45, 130.89, 128.8, 122.49, 98.07, 36.8. ESIMS: m/z 558 [M+AcOH]+.

Table 1. Structure and physical parameters of the synthesized quinazolinone derivatives

Entry	Compound Name	Structure	Molecular Formula	Molecular Weight	M. P. (0C)	Yield (%)
1	4a	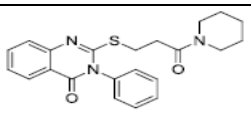	C22H23N3O2S	393	155-158	50
2	4b	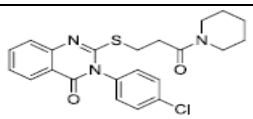	C22H22ClN3O2S	427	167-170	45

3	4c	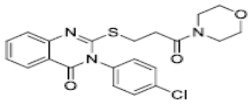	C21H20ClN3O3S	429	145-150	45
4	4d	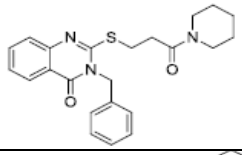	C23H25N3O2S	407	175-177	55
5	4e	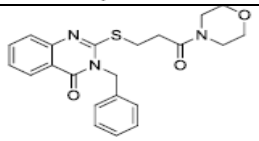	C22H23N3O3S	409	160-162	55
6	4f	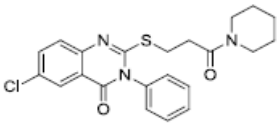	C22H22ClN3O2S	427	200-203	55
7	4g	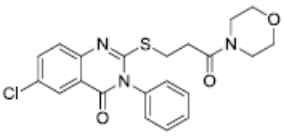	C21H20ClN3O3S	429	180-185	55
8	4h	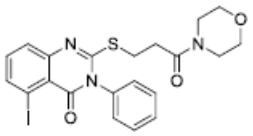	C21H20IN3O3S	521	140-143	55
9	4i	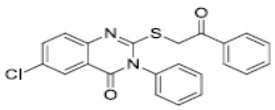	C22H15ClN2O2S	406	198-201	55
10	4j	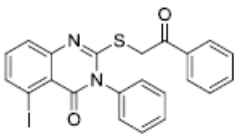	C22H15N2O2S	498	167-172	55

3.2 Molecular docking studies: To understand the ligand orientation and the inhibitory ability towards *human* Hsp90 (PDB ID: 1YET), we carried out docking of the synthesized quinazolinone derivative compounds using LibDock docking program. It produces several poses, each producing their corresponding docking scores with different orientations within the defined active site of the protein. The high LibDock score of the ligand pose was taken into account for the prediction of the best ligand binding conformation. So, the above pre-validated analysis was used to sort out the retrieved hit molecules and then those are further validated by using the visualization method to find the suitable binding mode of the inhibitors based on the critical interactions with the active site residues. Finally, the Analyze Ligand Poses sub protocol was performed to count Hbonds and close contacts (van der Waals clashes) between the poses and Hsp90. The Summary of docking information of the top ranked poses of each compound are tabulated in Table 2.

Docking analysis of 10 synthesized quinazolinone derivative compounds with the human Hsp90 revealed that the compound 4j fitted well in the active site pocket, showing the best docking score of 101.305. The best conformation with H-bond interactions obtained for compound 4j is shown in figure 2. From the Figure 1 it is revealed that a hydrogen bond is formed between iodine atom of compound 4j and the nitrogen atom of the amino acid Aspargine 93 with a hydrogen bond distance of 2.2070 Å. Some close contacts are also formed between the protein and the compound 10. They are formed with the iodine atom of comp 4j and the amino acid THR184 and hydrogen atom of comp 4j and the amino acid MET98 with a distances of 1.9100 Å and 1.6860 Å respectively.

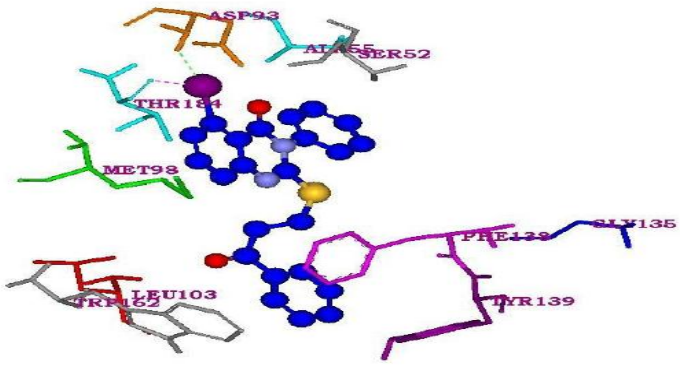

Figure 1. Receptor-ligand Hydrogen bonding interactions of compound 4j with the active site residues of Hsp90

Table 2. Docking summary of the synthesized molecules

Name	Libdock Score	Vander Waal energy	Electrostatic Energy	Interacting amino acids	Interacting atoms	H-bond Distance
4a	92.061	-0.33	2.518	Asp93,Gly135,Tyr139, Phe138, Ser52,Ala55,Tyr139,Thr184,Leu103, Trp162,Met98	A:TRP162:HE1-comp1.mol:O28 comp1.mol:H44-A:LEU103:CD2 comp1.mol:H38-A:TYR139:OH	2.2550 1.9820 1.7770
4b	81.304	2.401	1.069	Asp93,Gly135,Tyr139, Phe138,Ser52,Ala55, Tyr139,Thr184,Met98 Leu103,Trp162	A:TRP162:HN1-comp2.mol:O28 comp2.mol:H49-A:THR184:CG2	2.1770 2.0690
4c	86.298	5.609	1.218	Asp93,Gly135,Tyr139, Phe138,Ser52,Ala55, Tyr139,Thr184, Met98 Leu103,Trp162	A:SER52:HG - comp3.mol:O27 Comp3.mol:H50 - A:ASP93:OD2	2.6100 1.91500
4d	84.306	-1.608	2.544	Asp93,Gly135,Tyr139, Phe138,Ser52,Ala55, Tyr139,Thr184,Met98 Leu103,Trp162	A:SER52:HT2 - Comp4.mol:O24 Comp4.mol:H49 - A:SER52:N	2.2650 2.0240
4e	96.621	-10.246	1.771	Asp93,Gly135,Tyr139, Phe138,Ser52,Ala55, Tyr139,Thr184 Leu103,Trp162,Met98	A:PHE138:HN1 - comp5:O22 A:TRP162:NE1 - comp5:O21	1.8710 2.7980
4f	99.966	-4.895	0.729	Asp93,Gly135,Tyr139, Phe138,Ser52,Ala55, Tyr139,Thr184 Leu103,Trp162,Met98	A:TRP162:NE1 - comp6:O29 A:PHE138:HN1 - comp6:O28	2.8620 1.8700
4g	67.838	2.602	-5.123	Asp93,Gly135,Tyr139, Phe138,Ser52,Ala55, Tyr139,Thr184 Leu103,Trp162,Met98	A:PHE138:HN - Comp7:O11 A:TYR139:HE2 - Comp7:C14	2.0400 2.0880
4h	94.115	4.176	2.774	Asp93,Gly135,Tyr139, Phe138,Ser52,Ala55, Tyr139,Thr184 Leu103,Trp162,Met98	A:TRP162:HE1 - comp8:I24 A:SER52:HT2 - comp8:O26 comp8:C29 - A:ALA55:HB3	2.4730 2.3680 2.1110
4i	91.747	2.424	1.323	Asp93,Gly135,Tyr139, Phe138,Ser52,Ala55, Tyr139,Thr184 Leu103,Trp162,Met98	A:SER52:HG - comp9:O16 comp9:H32 - A:TRP162:CG	2.2990 2.0350
4j	101.305	4.332	-10.246	Asp93,Gly135,Tyr139, Phe138,Ser52,Ala55,Tyr139,Thr184,Leu103, Trp162,Met98	A:ASP93:HN1-Comp10:I23 A:THR184:O-Comp10:I23 comp10:H42 - A:MET98:HN1	2.2070 1.9100 1.6860

3.3. Validation of docking studies by structure based pharmacophore mapping

For a better understanding of the key features that are responsible for biological function of our compounds, structure based pharmacophore modeling was performed. The ligand interactions with the amino acid residues present in the active site was a suitable input to design the structure based pharmacophore model of our target protein *Human* Hsp90 (1YET). The Interaction Generation protocol constructed ten pharmacophore models comprising hydrogen bond acceptor (HBD), hydrogen bond donor (HBA) and hydrophobic features for our protein evaluating them based on their selectivity score, the higher the better was taken for further analysis. Using the Edit and Cluster Pharmacophore tool available in Discovery studio, the identified features are grouped and refined. The final edited pharmacophore model of Hsp90 (1YET) has two HBD, two HBA and two hydrophobic features. The generated structure based pharmacophore model was depicted in the Figure 2. For the assessment of the quality of the generated pharmacophore, the final pharmacophore model undergoes validation process in accordance with the active site coordination of our compounds. At this step, it was important to find candidate compounds that being able to fit in the generated structure-based pharmacophore model, which was a reflection of the active site geometry. Using Ligand Pharmacophore Mapping protocol, with the Best conformation generation and Flexible fitting methods, all the taken quinazolinone derivatives compounds are mapped on to the pharmacophore model. Geometric fit values are calculated for every compound hit based on how well the chemical substructures of a compound map on to the pharmacophoric feature location constraints. The best-fit value of the molecule to the respective pharmacophore was calculated.

Molecules are ranked based on their fit values computed and the compounds with high fit values are chosen for further studies. The fitness scores of the compounds with the pharmacophore model of Human Hsp90 (1YET) was shown in Table 3, ranging from 2.976 to 2.624. Here based on the fit scores, the compounds 4j fitted well on the generated pharmacophore with fit values of 2.976 (figure 3).

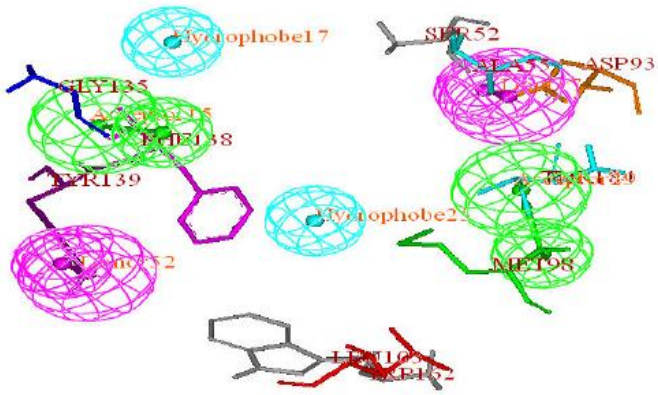

Figure 2. Generated structure based pharmacophore model of Human Hsp90 (PDB: 1YET) along with its active site pocket residues. Green color indicates hydrogen bond acceptor (HBA); cyan indicates hydrophobic (H) and magenta indicates hydrogen bond donor (HBD).

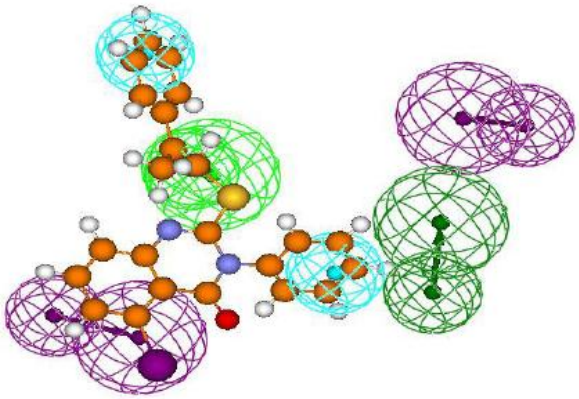

Figure 3. Ligand pharmacophore mapping of the high active compound 4j on to the structure based pharmacophore model

Table 3. The predicted fit values of the compounds from the structure based pharmacophore model of Human Hsp90

Name	Acceptor15	Acceptor29	Donor52	Donor7	FitValue	Hydrophobe17	Hydrophobe25
4j	1	0	0	0	2.976	1	1
4f	1	0	0	0	2.885	1	1
4i	1	0	0	0	2.883	1	1
4b	1	0	0	0	2.882	1	1
4e	1	0	0	0	2.871	1	1
4d	1	0	0	0	2.868	1	1
4c	1	0	0	0	2.867	1	1
4a	1	0	0	0	2.867	1	1
4h	1	0	0	0	2.727	1	1
4g	1	0	0	0	2.624	1	1

3.4. Malachite Green Assay for Hsp90 ATPase Activity: To characterize the inhibition of Hsp90 by the synthesized quinazolinone derivatives, a colorimetric malachite green assay for inorganic phosphate was used to measure the ATPase activity of Hsp90. The results are tabulated in Table 4. All the absorbance values were coinciding with the values obtained from the standard curve. From all the derivatives, compound 4j have shown least ATPase activity (high inhibition) with an IC50 value of 25 μM whereas the compound 4i showed the maximum ATPase activity(less inhibition) with an IC50 value of 64 μM.

3.5. In vitro cytotoxicity activity: The synthesized compounds were screened for in vitro cytotoxic activity using the micro culture tetrazolium assay, tested against human breast cancer line MCF-7. The various concentrations of the synthetic compounds (final concentration 5, 10, 20, 40, 80 and 100 μg/ml) were applied to calculate IC50. The 50% growth inhibitory concentration (IC50) for products were calculated and depicted in Table 1. From the Table 4 it is evident that the compound 4j showed the highest activity against MCF-7 cell lines with IC50 value of 97.71 μg/ml.

Table 4. Biological data for Hsp90 inhibitors

Test samples	Concentration of Hsp90 IC50 (μM)	In vitro Cytotoxicity on MCF-7 cell line IC50 (μM)
4a	27.5	166.14
4b	49	425.60
4c	25.5	116.04
4d	49	Not detected
4e	28.5	241.23
4f	25.3	Not detected
4g	26.7	Not detected
4h	25.7	460.31
4i	64	129.25
4j	25	97.71
Geldanamycin	5	9

4. CONCLUSION

In conclusion, all the synthesized quinazolinone derivatives were found to have Hsp90 ATPase inhibitory activity. Docking simulation of these inhibitors in the ATP binding site of Hsp90 showed a direct hydrogen bond with Asp93, which is considered a crucial binding force to stabilize enzyme-inhibitor complexes. The biological evaluation of in vitro cytotoxicity on MCF-7 cell lines and the Hsp90 ATPase inhibitory activity results revealed the compound 4j [5-iodo-2-((2-oxo-2-phenylethyl)thio)-3- phenylquinazolin4(3H)-one] shows maximum activity among the 10 synthesized derivatives. The performed computational docking and pharmacophore studies also predicted the same compound 4j as the most potent lead compound among the 10 synthesized compounds. In conclusion, compound 4j can serve as a promising lead for further chemical modification and optimization.

REFERENCES

1. Taipale M, Jarosz DF, Lindquist S. HSP90 at the hub of protein homeostasis: Emerging mechanistic insights. Nat Rev Mol Cell Biol 2010; 11: 515-28.
2. Prodromou C. Mechanisms of Hsp90 regulation. Biochemical Journal 2016; 473(16): 2439-52.
3. Finka A, Goloubinoff P. Proteomic data from human cell cultures refine mechanisms of chaperonemediated protein homeostasis. Cell Stress Chaperones 2013; 18: 591–605.
4. Tatokoro M, Koga F, Yoshida S, Kihara K. Heat shock protein 90 targeting therapy: state of the art and future perspective. EXCLI Journal 2015; 14: 48-58.

5. Trepel J, Mollapour M, Giaccone G, Neckers L. Targeting the dynamic HSP90 complex in cancer. Nat Rev Cancer 2010; 10: 537–549.
6. Jia J, Xu X, Liu F, Guo X, Zhang M, Lu M, et al. Identification, design and bio-evaluation of novel Hsp90 inhibitors by ligand-based virtual screening. PloS one 2013; 8(4): e59315.
7. Pratt WB, Morishima Y, Peng HM, Osawa Y. Proposal for a role of the Hsp90/Hsp70-based chaperone machinery in making triage decisions when proteins undergo oxidative and toxic damage. Experimental Biology and Medicine 2010; 235(3): 278-89.
8. Den RB, Lu B. Heat shock protein 90 inhibition: rationale and clinical potential. Therapeutic advances in medical oncology 2012; 4(4): 211-18.
9. Nahleh Z, Tfayli A, Najm A, El Sayed A, Nahle Z. Heat shock proteins in cancer: targeting the 'chaperones'. Future medicinal chemistry 2012; 4(7): 927-35.
10. Pillai RN, Ramalingam SS. Heat shock protein 90 inhibitors in non-small-cell lung cancer. Current opinion in oncology 2014; 26(2): 159-64.
11. Baby ST, Sharma S, Enaganti S, Cherian RP. Molecular docking and pharmacophore studies of heterocyclic compounds as Heat shock protein 90 (Hsp90) Inhibitors. Bioinformation 2016; 12(3): 149-55.
12. Shi J, Van de Water R, Hong K, Lamer RB, Weichert KW, Sandoval CM, et al. EC144 is a potent inhibitor of the heat shock protein 90. Journal of medicinal chemistry 2012; 55(17): 7786-95.
13. Chang DJ, An H, Kim KS, Kim HH, Jung J, Lee JM, et al. Design, synthesis, and biological evaluation of novel deguelin-based heat shock protein 90 (HSP90) inhibitors targeting proliferation and angiogenesis. Journal of medicinal chemistry 2012; 55(24): 10863-84.
14. Gupta SD, Snigdha D, Mazaira GI, Galigniana MD, Subrahmanyam CV, Gowrishankar NL, Raghavendra NM. Molecular docking study, synthesis and biological evaluation of Schiff bases as Hsp90 inhibitors. Biomedicine & Pharmacotherapy 2014; 68(3): 369-76.
15. Grover A, Shandilya A, Agrawal V, Pratik P, Bhasme D, Bisaria VS, Sundar D. Hsp90/Cdc37 Chaperone/co-chaperone complex, a novel junction anticancer target elucidated by the mode of action of herbal drug Withaferin A. BMC bioinformatics 2011; 12(1): S30.
16. Patki JM, Pawar SS. HSP90: Chaperone-me-not. Pathology & Oncology Research 2013; 19(4): 631- 40.
17. Pati B, Banerjee S. Quinazolines: an illustrated review. Journal of Advanced Pharmacy Education & Research 2013; 3(3): 136-51.
18. Saravanan G, Alagarsamy V, Prakash CR. Synthesis and evaluation of antioxidant activities of novel quinazoline derivatives. Int J Pharm PharmSci 2010; 2: 83–86.
19. Rohini R, Muralidhar Reddy P, Shanker K, Hu A, Ravinder V. Antimicrobial study of newly synthesized 6-substituted indolo[1,2-c]quinazolines. Eur J Med Chem 2010; 45: 1200–05.
20. Chen X, Wei H, Yin L, Li X: A convenient synthesis of quinazoline derivatives via cascade imimo- Diels-Alder and oxidation reaction. Chin ChemLett 2010; 21: 782–86.
21. Vijayakumar B, Prasanthi P, Teja KM, Reddy KM, Nishanthi P, Nagendramma M, Nishanthi M. Quinazoline derivatives and pharmacological activities: a review. International Journal of Medicinal Chemistry & Analysis 2013; 3(1): 10-21.
22. Paneersalvam P, Raj T, Ishar PS M, Singh B, Sharma V, Rather BA. Anticonvulsant activity of Schiff bases of 3-amino-6,8-dibromo-2-phenylquinazolin-4(3H)-ones. Indian J Pharm Sci 2010; 72: 375– 78.
23. Pandeya SN, Sriram D, Nath G, Clercq E D. Synthesis antibacterial antifungal and anti-HIV evaluation of Schiff and Mannich bases of isatin derivatives with 3-amino-2-methylmercapto quinazolin- 4(3H)-one. PharmaceuticaActaHelvetiae 1999; 74: 11–17.
24. Alagarsamy V, Parthiban P. Design and Synthesis of Novel 3-(Phenyl)-2-(3-substituted propylthio) Quinazolin-4-(3H)-ones as a New Class of H1-Antihistaminic Agents. Journal of Heterocyclic Chemistry. 2014; 51(6): 1615-20.
25. Raffa D, Daidone G, Maggio B, Cascioferro S, Plescia F, Schillaci D. Synthesis and antileukemic activity of new 3-(5-methylisoxazol-3-yl) and 3-(pyrimidin-2-yl)-2-styrylquinazolin-4 (3H)-ones. IL Farmac. 2004; 59: 451–55.
26. Wang F, Zhao P, Xi C. Copper-catalyzed one-pot synthesis of 2-thioxo-2, 3-dihydroquinazolin-4 (1H)-ones from ortho-bromobenzamides and isothiocyanates. Tetrahedron letters 2011; 52(2): 231-35.
27. Nagwa M A G, Hanan H G, Riham M Y, Nehad A E S. Synthesis and antitumor activity of some 2, 3-disubstituted quinazolin-4(3H)-ones and 4,6-disubstituted-1,2,3,4-tetrahydroquinazolin-2H-ones. European Journal of Medicinal Chemistry 2010; 45: 6058-67.
28. Alagarsamy V, Parthiban P. Design and Synthesis of Novel 3-(Phenyl)-2-(3-substituted propylthio) Quinazolin-4-(3H)-ones as a New Class of H1-Antihistaminic Agents. Journal of Heterocyclic Chemistry 2014; 51(6): 1615-20.
29. Mohamed MA, Ayyad RR, Shawer TZ, Alaa AM, El-Azab AS. Synthesis and antitumor evaluation of trimethoxyanilides based on 4 (3H)-quinazolinone scaffolds. European journal of medicinal chemistry 2016; 112: 106-13.
30. Maehama T, Taylor GS, Slama JT, Dixon JE. A sensitive assay for phosphoinositide phosphatases. Analytical biochemistry 2000; 279(2): 248-50.

31. Henkel RD, VandeBerg JL, Walsh RA. A microassay for ATPase. Anal Biochem 1988; 169: 312–318.
32. Sylvester PW. Optimization of the tetrazolium dye (MTT) colorimetric assay for cellular growth and viability. Methods Mol Biol 2011; 716: 157–68.
33. Scudiero DA, Shoemaker RH, Paull KD, Monks A, Tierney S, Nofziger TH, et al. Evaluation of a soluble tetrazolium/formazan assay for cell growth and drug sensitivity in culture using human and other tumor cell lines. Cancer Res 1988; 48: 4827–33.
34. Marshall NJ, Goodwin CJ, Holt SJ. A critical assessment of the use of microculture tetrazolium assays to measure cell growth and function. Growth Regul 1995; 5: 69–84.
35. Brooks BR, Bruccoleri RE, Olafson BD: CHARMM: A program for macromolecular energy, minimization, and dynamics calculations. J Comput Chem 1983; 4: 187-217.
36. Berman HM, Battistuz T, Bhat TN, Bluhm WF, Bourne PE, Burkhardt K, Feng Z, Gilliland GL, Iype L, Jain S, Fagan P. The protein data bank. Acta Crystallographica Section D: Biological Crystallography. 2002; 58(6): 899-907.
37. Rao SN, Head MS, Kulkarni A, LaLonde JM. Validation studies of the site-directed docking program LibDock. J Chem Inf Model 2007; 47: 2159–71.
38. Böhm HJ. The computer program LUDI: a new method for the de novo design of enzyme inhibitors. Journal of computer-aided molecular design 1992; 6(1): 61-78.